

SUMMARY

We examine “polaroastrometry” – a novel technique for obtaining polarization information of astronomical objects below diffraction limited resolution, as a tool for investigation of the parsec scale structure in the jets of blazars. Optical polaroastrometry is based on measurements of differences between centroids of orthogonally polarized images. Recently the accuracy of 60-70 μas (in terms of 1σ) of polaroastrometric signal determination has been reached with a 70-cm telescope. We consider a two component model of blazars, which is able to explain rotations of the electric vector position angle (EVPA) and the long-term polarization variability observed in the optical emission. Using this model we estimate an expected polaroastrometric signal during two EVPA rotation events. According to the simulations the polaroastrometric signal can be potentially detected with a large telescope (6-8 meter class). Thereby we can obtain a new type of observational evidence to discriminate between existing models of the EVPA rotations in blazars.

EVPA ROTATIONS IN BLAZARS

Typically variability of polarization in blazars is erratic. However occasionally they exhibit smooth and monotonic rotations of the EVPA in the optical band. These rotations are often coincident with prominent flares observed at different frequencies. A number of mechanisms has been proposed to explain rotations of the EVPA. Most of them include an emission feature traveling down the jet at an ultrarelativistic speed. This emission feature can produce an EVPA rotation accompanied by a multiwavelength flare either due to the motion along a curved streamline following the helical magnetic field (Marscher et al. 2010; Larionov et al. 2013) or due to the bend in the jet (Abdo et al. 2010) or due to disturbances produced in the jet (Zhang et al. 2014). On the other hand Marscher et al. (2010) showed that the end of the rotation in Fig. 2 was coincident with a passage of a knot through the radiocore at 43 GHz. This kind of radiocores are thought to be stationary emission features in the jet, that produce both radio and optical emission with a similar direction of polarization (Gabuzda et al. 2006; Algaba et al. 2011). Therefore **rotation duration \leq travel time of the moving feature until the standing shock**.

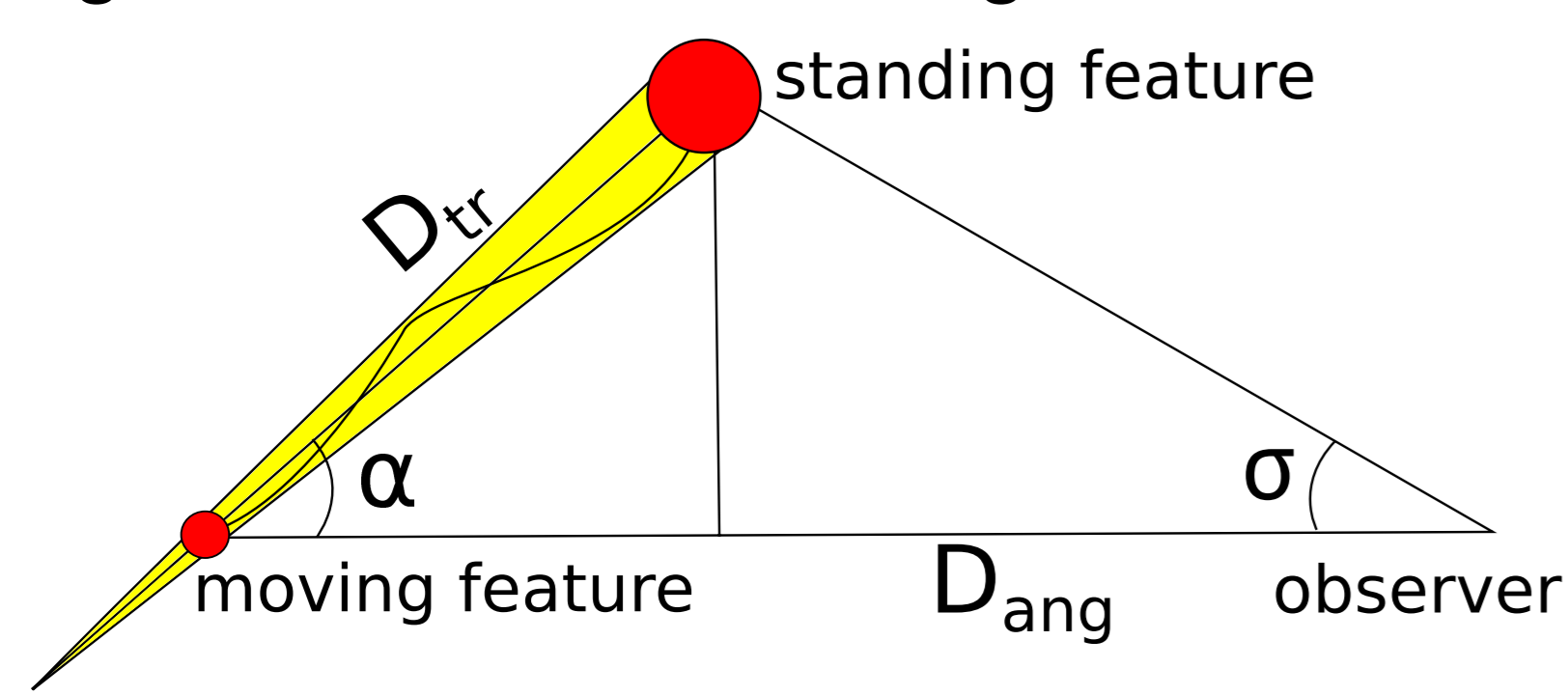


Figure 1: Model: emission feature traveling through the jet

Then σ traveled by the emission feature can be from the duration of the rotation in the observer's frame T_{tr} :

$$\sigma = \arctan\left(\frac{D_{tr} \sin \alpha}{D_{ang}}\right) \approx \arctan\left(\frac{c\Gamma^2 T_{tr} \sin \alpha}{D_{ang}}\right), \quad (1)$$

where $D_{tr} \approx c\Gamma^2 T_{tr}$ is the distance traveled by the emission feature during the rotation (Abdo et al. 2010), Γ - bulk Lorentz factor, α - viewing angle of the jet, D_{ang} - angular-size distance to the blazar.

We estimated σ for two EVPA rotations shown in Fig. 2 and Fig. 3.

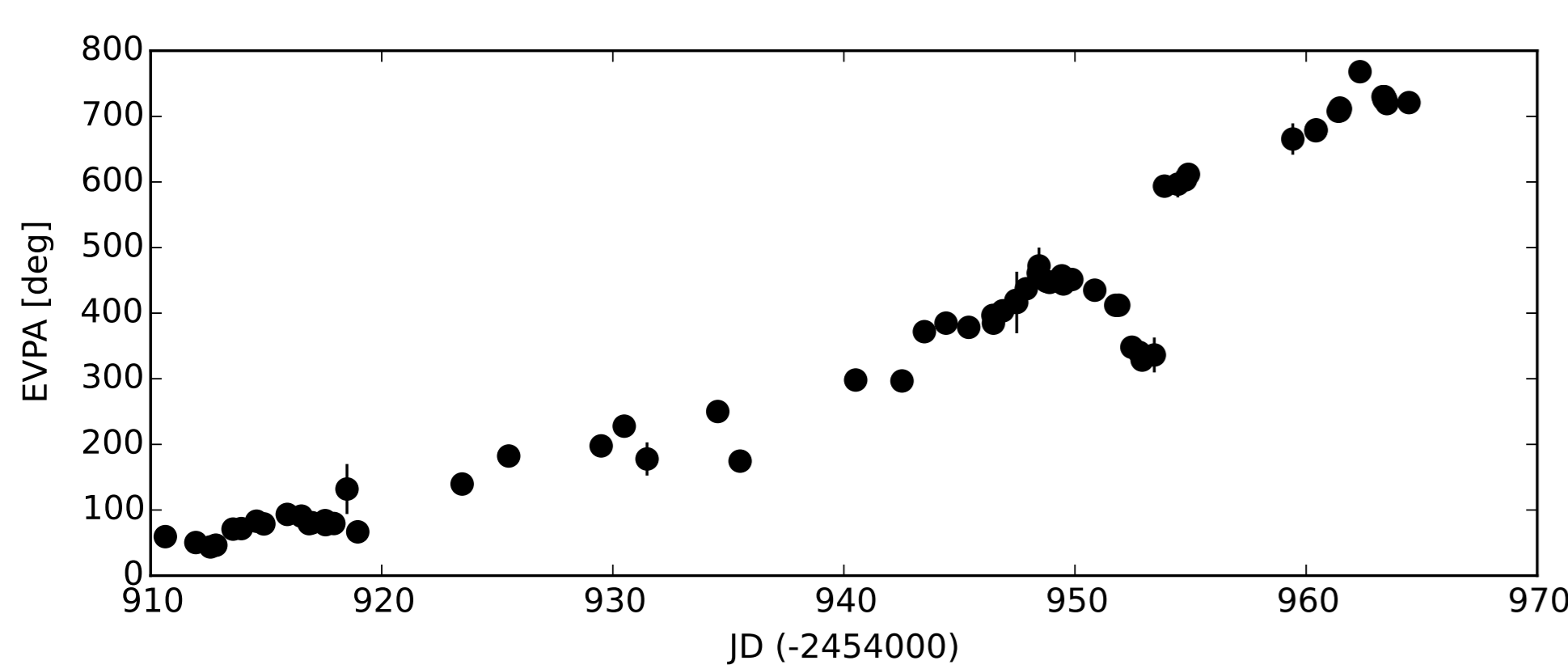


Figure 2: EVPA rotation in PKS 1510-089 (Marscher et al. 2010).

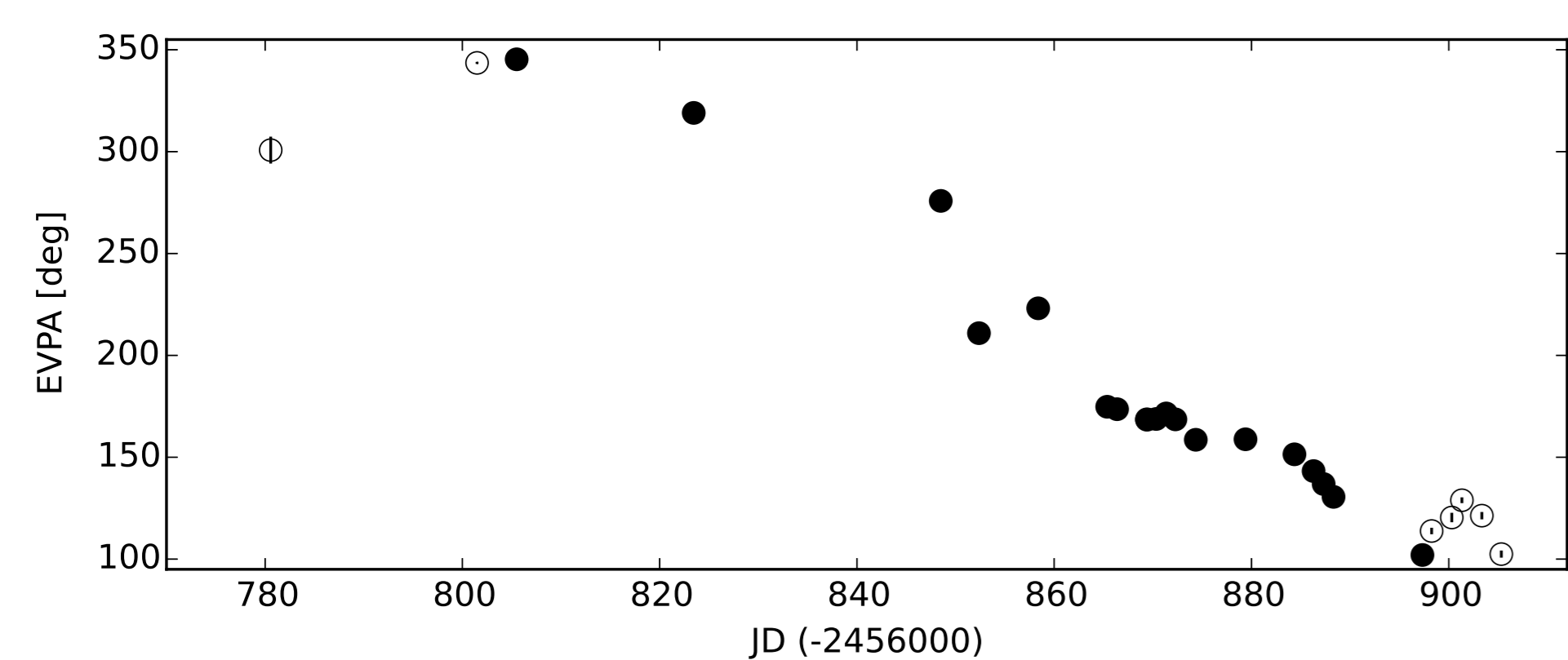


Figure 3: EVPA rotation in S4 1749+70 (Lioudakis 2014).

In both cases $\sigma < 1$ milliarcsec.

Table 1: Parameters of blazars and derived σ .

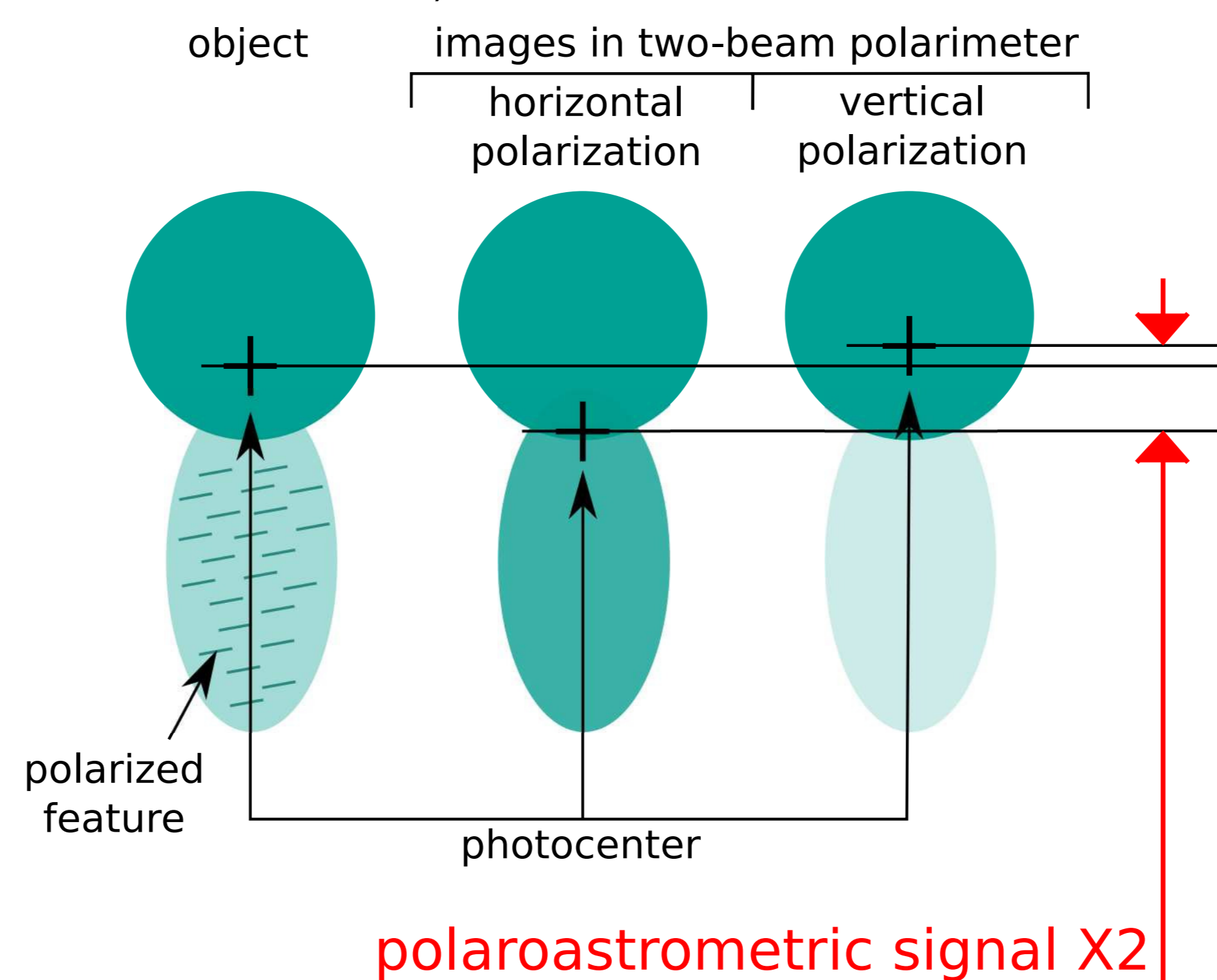
Parameter	PKS 1510-089	S4 1749+70
α (deg)	3.4 ¹	5.2 ⁵
T_{tr} (days)	50 ²	100
D_{ang} (Mpc)	1005 ³	1488 ³
Γ	36.6 \pm 7.0 ⁴	10.3 ⁵
σ (μas)	448 – 971	112

¹Hovatta et al. (2009); ²Marscher et al. (2010); ³NED; ⁴Jorstad et al. (2005);

⁵average value for BL Lacs from Hovatta et al. (2009)

POLAROASTROMETRY

Polaroastrometry – subdiffraction limited resolution of polarized components in objects. (Safonov 2013; Johnson et al. 2014)



The idea of polaroastrometry is to measure a half-difference between photocenters of horizontally and vertically polarized images – polaroastrometric signal. The polaroastrometric signal is a vector and can be defined for Stokes parameters Q, U, V .

We tested the polaroastrometry using frames obtained using a two-beam polarimeter with half-wave plate (Safonov 2015), see Fig. 4. Horizontally and vertically polarized images are obtained simultaneously on the same detector, thus eliminating many instrumental effects generating noise. The rest of systematic effects are mitigated by switching of the images with the HWP.

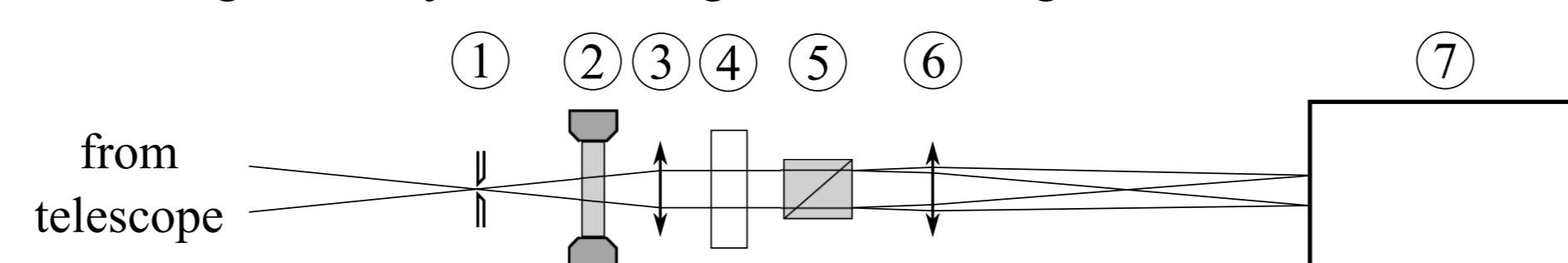


Figure 4: Scheme of the instrument used in the experiment. Numbers are for the components: 1) field diaphragm; 2) half-wave plate; 3) collimator lens; 4) filter; 5) Wollaston prism; 6) camera lens; 7) detector.

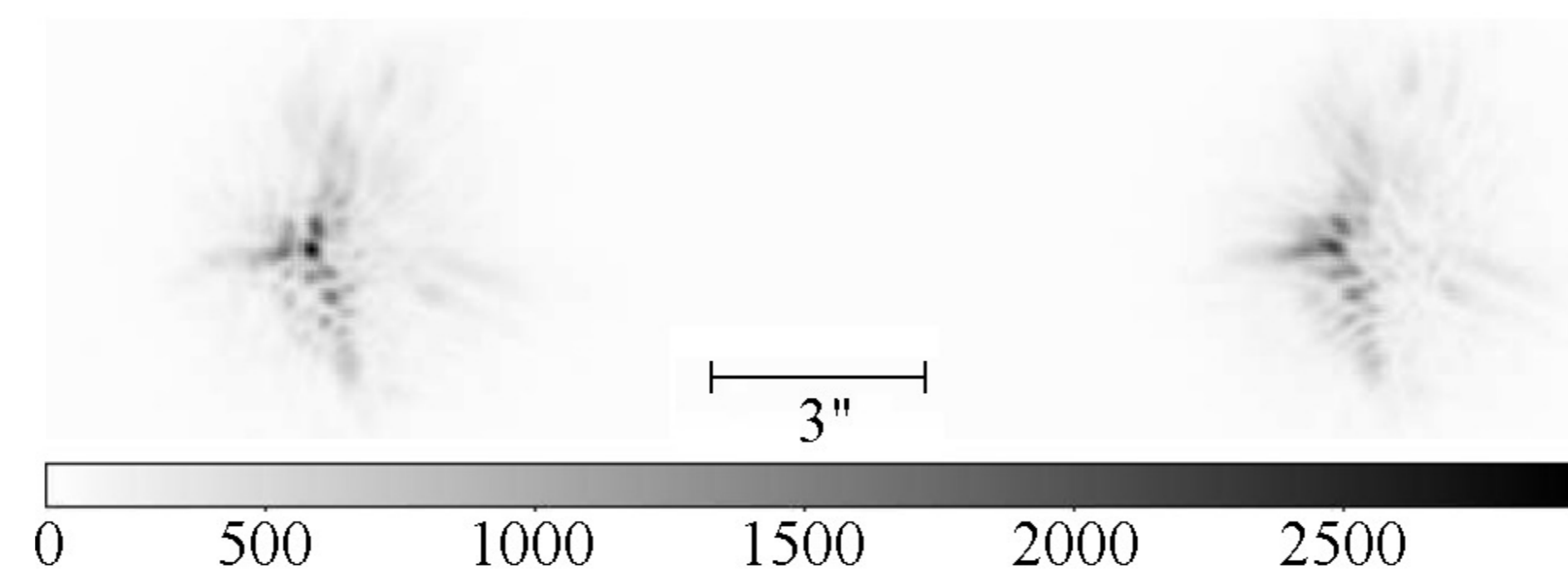


Figure 5: Single frame with α Lyr obtained with two-beam polarimeter.

As test objects we observed several main sequence stars, unpolarized and polarized by interstellar dust, which have presumably very small polaroastrometric signal. On the contrary, asymmetric dusty envelopes of Mira type variables χ Cyg and σ Cet, scattering radiation of photosphere, are expected to generate a detectable signal. Observations confirm these suggestions (Safonov 2015), see Tab. 2. **For these measurements we achieved polaroastrometry noise of 60-70 μas using a 70-cm telescope, which is 2000 \times times smaller than its diffraction limit.**

Table 2: Polarostrometric signal and dimensionless Stokes parameters for some of observed objects.

Parameter	HD186882	HD204827	χ Cyg	σ Cet
$q \times 10^4$	0.8 \pm 0.5	-258.2 \pm 5.3	-22.5 \pm 0.8	-1.5 \pm 0.7
$\Delta_{a,x}$ (μas)	+20 \pm 30	+90 \pm 120	+230 \pm 90	-150 \pm 110
$\Delta_{a,y}$ (μas)	+10 \pm 50	+110 \pm 120	+210 \pm 80	-470 \pm 100
$u \times 10^4$	0.8 \pm 0.5	483.0 \pm 3.2	-28.9 \pm 0.7	-28.9 \pm 0.7
$\Delta_{u,x}$ (μas)	+40 \pm 30	+20 \pm 120	-50 \pm 90	+890 \pm 110
$\Delta_{u,y}$ (μas)	+0 \pm 50	+50 \pm 120	-240 \pm 80	-790 \pm 100

Achieved level of noise is still 10 times greater than expected due to instrumental factors: half-wave plate imperfection, telescope aberrations, atmospheric dispersion and Wollaston prism dispersion. After mitigation of these factors a photon noise limit of astrometry will become achievable.

BLAZAR POLAROASTROMETRY: EXPECTATIONS

Assuming the two component model for both rotations in Fig. 2, 3 we estimated expected polaroastrometric signal for each observing point, results are in Fig. 6. Also we give there the photon noise limit for 2.5-m and 6-m telescope.

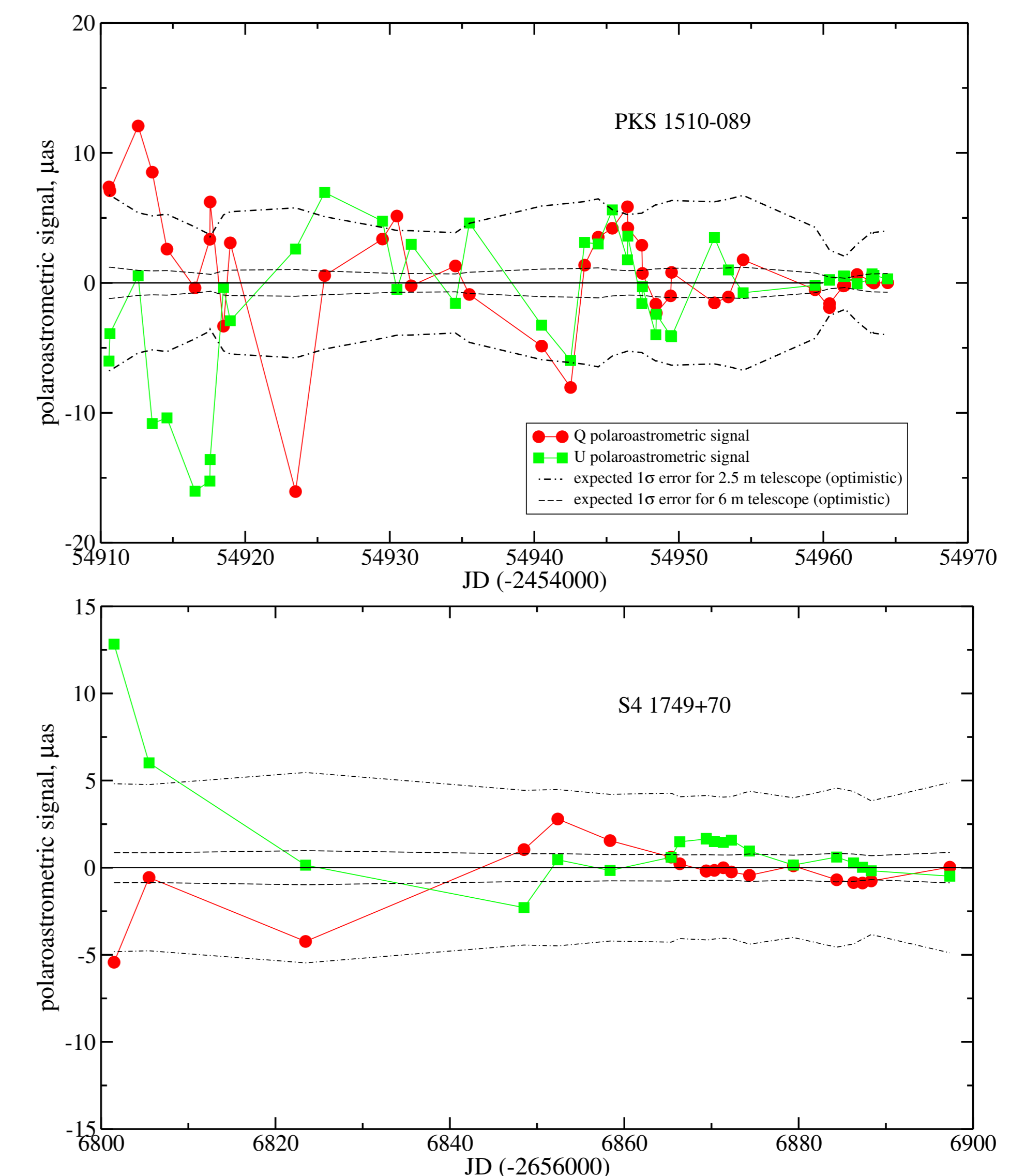


Figure 6: Simulated polaroastrometric signal for PKS 1510-089 and S4 1749+70 in R band. Red circles are for the Q component, green squares – for the U component. Dash-dotted and dashed lines are expected 1σ error level for observations with 2.5-m and 6-m telescope, respectively, total integration time 1 hour.

As one can see, 2.5-m telescope may marginally detect the signal, but reliable conclusion should be made with a larger instrument, 6-m or 8-m class.

CONCLUSION

The polaroastrometric signal can be detected during an EVPA rotation consistent with the two component model. If rotations are produced by a random walk, the signal will be below the noise limit. Thereby we can discriminate between these models. In case of validity of the first model the polaroastrometry potentially allows us to determine the doppler factors of the moving emission features upstream the radiocore and the direction of its motion.

REFERENCES

- Abdo, A. A., Ackermann, M., Ajello, M., et al. 2010, Nature, 463, 919
 Algaba, J. C., Gabuzda, D. C., & Smith, P. S. 2011, MNRAS, 411, 85
 Gabuzda, D. C., Rastorgueva, E. A., Smith, P. S., & O'Sullivan, S. P. 2006, MNRAS, 369, 1596
 Hovatta, T., Valtaoja, E., Tornikoski, M., & Lähteenmäki, A. 2009, A&A, 494, 527
 Johnson, M. D., Fish, V. L., Doeleman, S. S., et al. 2014, ApJ, 794, 150
 Jorstad, S. G., Marscher, A. P., Lister, M. L., & et al. 2005, AJ, 130, 1418
 Larionov, V. M., Jorstad, S. G., Marscher, A. P., et al. 2013, ApJ, 768, 40
 Lioudakis, I. 2014, ATel, 6351, 1
 Marscher, A. P., Jorstad, S. G., Larionov, V. M., Aller, M. F., & et al. 2010, ApJL, 710, L126
 Safonov, B. 2015, ArXiv:1501.03807
 Safonov, B. S. 2013, AstL, 39, 237
 Zhang, H., Chen, X., & Böttcher, M. 2014, ApJ, 789, 66

CONTACTS

Boris Safonov: safonov10@gmail.com
 Dmitry Blinov: blinov@physics.uoc.gr

